Indian J. Phys. **70A** (3) 393–412 (1996)

IJP A
– an international journal

THE TOP STORY

D.P. Roy
Tata Institute of Fundamental Research
Homi Bhabha Road, Bombay - 400 005, India

Abstract: This is an overview of top quark search, with particular emphasis on the more recent results. After a brief introduction to the basic constituents of matter and their interactions, I shall discuss the indirect evidences for the existence of top quark and its mass from LEP and finally the direct observation of a top quark signal recently reported from the Tevatron collider. I shall try to put these results in perspective and provide some insight into the physics issues involved in the top quark search.

Keywords: top quark, electroweak theory, colliders

PACS Nos: 12.15.Ff, 14.65.Ha

1 Basic Constituents of Matter and their Interactions

As per our current wisdom the basic constituents of matter are a dozen of fermions : the six leptons – electron, muon, tau and their associated neutrinos; and the six quarks – up, down, strange, charm, bottom and top. They can be arranged as three pairs or generations of leptons and quarks, which are shown below in increasing order or mass.

Table 1

Leptons	Q	T^3	Quarks	Q	T^3
$\nu_e\ \nu_\mu\ \nu_\tau$	0	1/2	$u\ c\ t$	2/3	1/2
$e\ \ \mu\ \ \tau$	-1	-1/2	$d\ s\ b$	-1/3	-1/2

Each pair represents two states differing by 1 unit of electric charge Q, which correspond to the two eigenstates of weak isospin $T^3 = \pm 1/2$. In addition, the quarks possess a new type of charge called the colour charge, which is responsible for their strong interaction.

Many of these fundamental particles, the τ lepton and the charm and bottom quarks, were discovered during the seventies. Thus by the end of the seventies all of them had been seen except for the last and the heaviest one – i.e. the top quark. Consequently the top quark search has been an area of intense activity since the early eighties. The evidence for top has built up step by step from many indirect experiments during this period, culminating in the direct observation of a top quark signal recently reported from the Tevatron collider. I shall give an overview of this top search programme, concentrating on the more recent results. To facilitate this discussion and fix the notation let me briefly recall the basic interactions between these fundamental particles.

Apart from gravitation, which is too weak to be of interest to our discussion of subatomic particles, there are 3 basic interactions – strong, electromagnetic and weak. They are all gauge interactions mediated by vector particles with couplings proportional to the corresponding gauge charge. The strong interaction (QCD) is mediated by the exchange of massless vector gluons, which couple to all coloured particles (quarks) with coupling proportional to the colour charge C (Fig. 1a). This is analogous to the electromagnetic interaction (QED), mediated by the exchange of massless vector photon, which couples to all charged particles (quarks and charged leptons) with coupling proportional to the electric charge Q (Fig. 1b). It is customary to write the strong coupling constant as

$$\alpha_s = g_s^2/4\pi \tag{1}$$

in analogy with the fine structure constant

$$\alpha = e^2/4\pi. \tag{2}$$

The weak interactions are mediated by the massive charged and neutral vector bosons $W^{\pm}$ and Z^0. The charged W boson couples to each of the above pairs of quarks and leptons with the same universal coupling g (Fig. 1c), where the combination of the Dirac γ matrices correspond to the famous $V - A$ (Lefthanded) form of the charged current weak interaction corresponding to the gauge group $SU(2)_L$. The neutral Z boson

couples to each quark and lepton (Fig. 1d) with couplings specified by the standard electro-weak model of Glashow, Weinberg and Salam. Here the weak and electromagnetic interactions are unified into a $SU(2)_L \times U(1)$ gauge interaction, mediated by a charge triplet of gauge bosons $W^{\pm,0}$ with couplings proportional to the three $SU(2)$ generators $T^{\pm,3}$ (weak isospin) and a charge singlet B^0 with coupling proportional to the $U(1)$ generator (weak hypercharge). The two neutral bosons get mixed to give the physical Z boson and photon. It is customary to use the $SU(2)$ coupling g and the mixing angle θ_W as the two independent parameters. Then the physical Z coupling is given by [1]

$$\frac{g}{\cos\theta_W}\left[T^3\gamma^\mu\frac{(1-\gamma^5)}{2} - \sin^2\theta_W Q\gamma^\mu\right] \tag{3}$$

and the physical photon coupling is related to these parameters by

$$g = e/\sin\theta_W. \tag{4}$$

The universality of the charged W coupling is of course a simple reflection of the fact that all the fermions appear in identical (doublet) representations of the weak isospin group $SU(2)$; i.e. they all possess the same $SU(2)$ charge.

In the standard model the $SU(2)$ gauge symmetry is spontaneously broken by the Higgs mechanism to give masses to the W and Z bosons as well as the fermions. Since the W and Z bosons acquire their masses and hence longitudinal components by absorbing the Higgs scalars, the longitudinal W and Z bosons have Higgs like Yukawa couplings to the fermions that are proportional to the corresponding fermion masses. This is important in the case of top quark due to its large mass; and we shall see later that it plays a crucial role in the indirect estimate of the top quark mass. On the other hand the W and Z boson interactions with all the lighter fermions are adequately described by the gauge couplings of (3,4), which are unaffected by the symmetry breaking. This plays an important role in extracting indirect evidence for the existence of top quark, as we see below.

2 Indirect Evidence for the Existence of Top Quark

As we see from (3), the Z boson coupling to bottom quark depends sensitively on its isospin T_b^3, which is $-1/2$ or 0 depending on whether

it is accompanied by a top quark as its isospin partner or not. Thus a measurement of the Z boson coupling to the bottom quark can distinguish between the two alternatives. There are a number of indirect evidences for the existence of top quark, based on this principle. They come from 1) the forward-backward asymmetry observed in $e^+e^- \to \bar{b}b$ at PETRA energy [2]; 2) the absence of flavour changing neutral current decay of b quark [3] as measured at CESR [4]; 3) the absence of large (tree-level) $B_d - \bar{B}_d$ mixing [5] as measured at DORIS and CESR [6]; and finally 4) the direct measurement of the $Z \to \bar{b}b$ width at LEP [7]. We shall concentrate on the last process, which provides by far the cleanest and strongest indirect evidence for top [8]. A comprehensive account of all the four processes can be found in [9].

The $Z \to \bar{b}b$ decay width has been measured to good precission at LEP giving [7]

$$\Gamma(Z \to \bar{b}b) = 385 \pm 6 \text{ MeV}. \tag{5}$$

¿From the $Z\bar{b}b$ coupling of (3), one can easily estimate this quantity to be [8]

$$\Gamma(Z \to \bar{b}b) = \frac{G_F M_Z^3}{\sqrt{2}\pi}\left(1 + \frac{\alpha_s}{\pi}\right)\left[\left(T_b^3 - Q_b \sin^2\theta_W\right)^2 + \left(Q_b \sin^2\theta_W\right)^2\right] \tag{6}$$

including the small QCD correction. The effective Fermi coupling [7]

$$G_F = \frac{\sqrt{2}g^2}{8M_W^2} = 1.166 \times 10^{-5} \text{ GeV}^{-2}. \tag{7}$$

Thanks to the small values of $\sin^2\theta_W$ and the b quark charge, the width depends crucially on the isospin assignment of b. One gets

$$\Gamma(Z \to \bar{b}b) = 381 \text{ MeV } (24 \text{ MeV}) \text{ for } T_b^3 = -\frac{1}{2}(0). \tag{8}$$

Comparing these predictions with the experimental width of (5), we see that the latter provides a very strong evidence of $\sim 60\sigma$ for the existence of a top quark as isospin partner of b.

It may be noted here that the first three evidences are also based on the T_b^3 dependence of the $Z\bar{b}b$ coupling. But they are all low energy processes, probing the effects of $Z\bar{b}b$ coupling far from the Z mass shell. Thus the

effects could be mimicked e.g. by other gauge bosons (Z') occurring in some extensions of the standard model gauge group [8]. There is no such ambiguity, however, for the on-shell $Z\bar{b}b$ coupling as measured by the decay width (5).

3 Indirect Estimate of the Top Quark Mass

There are several indirect constraints on the top quark mass. The experimental value of the $B_d - \bar{B}_d$ mixing [6], which is dominated by the top quark exchange box diagram, gives a lower mass limit [10]

$$m_t \gtrsim 60 \text{ GeV}. \tag{9}$$

A similar lower limit is also obtained from an indirect estimate of the W boson width at the Tevatron collider [7,11],

$$\Gamma_W = 2.06 \pm .06 \pm .06 \text{ GeV}, \tag{10}$$

which is completely saturated by the lighter fermion contributions, i.e.

$$\Gamma_W = \underbrace{\frac{G_F M_W^3}{6\sqrt{2}\pi}}_{0.23 \text{ GeV}} \left[e\bar{\nu} + \mu\bar{\nu} + \tau\bar{\nu} + 3\left(1 + \frac{\alpha_s}{\pi}\right)(d\bar{u} + s\bar{c})\right]. \tag{11}$$

More importantly there is an upper limit on top quark mass,

$$m_t \lesssim 200 \text{ GeV}, \tag{12}$$

coming from the radiative corrections to W and Z masses [12]. More over the precission measurement of these radiative correction effects at LEP has recently sharpened this constraint into an indirect estimate of m_t [13]. Therefore we shall discuss this result in some detail.

The W mass can be easily calculated at the tree level from the muon decay diagram of Fig. 1c, and the corresponding Z mass from the tree level relation[1]

$$M_Z = M_W / \cos\theta_W. \tag{13}$$

[1]This relation shall continue to be used as a working definition of $\sin^2\theta_W$ in the presence of radiative corrections.

The observed rate of muon decay gives a precise estimate of the Fermi coupling

$$G_F = \frac{g^2\sqrt{2}}{8M_W^2} = \frac{\pi\alpha}{\sqrt{2}\sin^2\theta_W M_W^2}, \tag{14}$$

quoted in (7). The mixing angle, as estimated from the neutrino scattering experiments [7], is

$$\sin^2\theta_W = .226 \pm .005. \tag{15}$$

Finally the EM coupling α at the appropriate mass scale is

$$\alpha(M_Z^2) = \alpha(m_e^2)[1 + \Delta r] \simeq 1/128, \tag{16}$$

corresponding to a EM radiative correction of $\Delta r \simeq .07$.[2] From (7) and (13-16) one gets,

$$M_W = 81.2 \pm 0.8 \text{ GeV}, \quad M_Z = 92.2 \pm 0.9 \text{ GeV} \tag{17}$$

compared to the experimental values [7] of

$$M_W = 80.1 \pm 0.4 \text{ GeV}, \quad M_Z = 91.19 \pm 0.01 \text{ GeV}. \tag{18}$$

The 1% uncertainty in the tree level predictions of M_W and M_Z are simply reflections of the 2% uncertainty in the $\sin^2\theta_W$ input (15). The predictions are higher than the corresponding experimental values by 1σ. Consider now the weak radiative corrections to M_W and M_Z. For large m_t, the dominant corrections come from the $t\bar{b}$ loop contribution to the W propagator (Fig. 2) and the analogous $t\bar{t}$ contribution to the Z. The reason is the large Yukawa couplings of longitudinal W and Z bosons to top quark, which are proportional to m_t as remarked earlier. The resulting radiative correction is $\propto m_t^2$, i.e.

$$M_W^2 = \frac{\pi\alpha(M_Z^2)}{\sqrt{2}\sin^2\theta_W G_F}(1 + \Delta r'), \tag{19}$$

$$\Delta r' \simeq \frac{-3\sqrt{2}}{16\pi^2} G_F \cot^2\theta_W m_t^2 \simeq -1.07 \times 10^{-6} m_t^2. \tag{20}$$

[2]To be more precise $\alpha(M_Z^2) \simeq 1/128.8$ [13], corresponding to a EM radiative correction of $\sim$ 6%. But there is a small radiative correction of $\sim$ 1% coming from weak processes other than the top quark exchange term ($\Delta r'$) discussed below [14].

Thus for $m_t > 200$ GeV one gets

$$\Delta r' < -.043 \Rightarrow M_W < 79.5 \pm 0.8 \text{ GeV}, \; M_Z < 90.2 \pm 0.9 \text{ GeV}, \quad (21)$$

i.e. a large negative radiative correction that pushes down M_Z below the experimental value by at least 1σ. Consequently one gets the upper limit of (12).

Fig. 3 shows a more exact calculation of the radiative correction as a function of m_t for two extreme values of the Higgs mass [14]. It has a mild (logarithmic) dependence on the latter. The 1σ bounds obtained from the experimental values of M_Z and $\sin^2\theta_W$ are shown separately for the cases where $\sin^2\theta_W$ is estimated from neutrino scattering (15) or from M_W/M_Z (18). In either case the favoured value of the radiative correction is $\Delta r' \simeq -.03$ corresponding to $m_t \simeq 170$ GeV. But the size of the error bar, which reflects the uncertainty in the estimate of $\sin^2\theta_W$, is too large to give a precise estimate of m_t. Recently it has been possible to pin down m_t or equivalently the $\sin^2\theta_W$ more precisely from a global fit to the precission measurements of the Z parameters at LEP [13]. It gives

$$m_t = 173^{+12}_{-13} \quad {}^{+18}_{-20}\text{GeV}, \quad (22)$$

or equivalently

$$\sin^2\theta_W = .2249 \pm .0013^{+.0003}_{-.0002}, \quad (23)$$

where the second errors correspond to varying M_H from 1000 GeV (upper) to 60 GeV (lower). This result is shown as a hatched band in Fig. 3. Note that the width of this band, or equivalently the 1st error bar of (22), corresponds to the uncertainty in the estimate of m_t related to that of $\sin^2\theta_W$. This uncertainty is now very small; but there is a somewhat larger uncertainty coming from the unknown Higgs mass. Consequently the overall uncertainty in the indirect estimate of m_t from LEP is somewhat larger than the direct estimate from the CDF experiment; but there is remarkably good agreement between the two results.

4 Direct Top Quark Search at the Electron-positron Collider

The e^+e^- collider can provide the cleanest signal for top quark; but unfortunately the energies are too low. The simplest way to look for

$e^+e^- \to \bar{t}t$ (Fig. 1b) is through the ratio of cross-sections

$$R = \frac{\sigma(e^+e^- \to \text{hadrons})}{\sigma(e^+e^- \to \mu^+\mu^-)} = \frac{\sigma(e^+e^- \to \Sigma\bar{q}q)}{\sigma(e^+e^- \to \mu^+\mu^-)} \simeq 3\sum Q_q^2, \qquad (24)$$

which should show a jump of $\Delta R = 3Q_t^2 = 4/3$ units across the $\bar{t}t$ threshold. One can readily check that this corresponds to an increase of the hadronic cross-section or R by about one third. The second way is to look at the event shape. The lighter quark pairs fly off back to back carrying the total centre of mass energy and thus give rise to highly collinear events. In contrast, near the $t\bar{t}$ threshold, the heavy t quark pair will be produced practically at rest; and each will decay into 3 quarks (Fig. 1c)

$$t \to bu\bar{d}, bc\bar{s}. \qquad (25)$$

Thus the total centre of mass energy would be shared amongst the 6 light quarks, giving rise to a more spherical (isotropic) event.

The PETRA and TRISTAN colliders have looked for $e^+e^- \to \bar{t}t$ events using these methods and found none. Thus they give lower bounds on top quark mass equal to their respective beam energies. The larger one, coming from TRISTAN [15] is $m_t > 26$ GeV. More recently the LEP e^+e^- collider has increased this mass bound to [16]

$$m_t > 45 \text{ GeV}, \qquad (26)$$

which corresponds to its beam energy. With the LEP-II, scheduled for the late nineties, the probe can be further extended upto its beam energy of about 90 GeV. As we have already seen, however, this is not large enough.

5 Direct Top Quark Signal at the Antiproton-proton Collider

The $\bar{p}p$ collider is best suited for a heavy top quark search because of its higher energy reach. But the signal is messy; and one has to use special techniques to disentangle it from the background. The dominant mechanism for top quark production is the so-called flavour creation process of gluon-gluon fusion (Fig. 4) and quark-antiquark fusion (Fig. 1a), i.e.

$$gg(\bar{q}q) \to \bar{t}t. \qquad (27)$$

The best way to look for top is to look for a prompt charged lepton ℓ (i.e. e or μ) coming from its leptonic decay

$$t \to b\nu\ell \tag{28}$$

as per Fig. 1c. This eliminates the background from gluon and ordinary stable quarks (u, d, s). Of course the charged lepton could come from the unstable quarks b and c i.e.

$$gg(\bar{q}q) \to \bar{b}b, \bar{c}c;$$

$$b \to c\nu\ell, \; c \to s\nu\ell. \tag{29}$$

These background can be effectively suppressed by requiring the charged lepton to be isolated from the other particles. Because of the large energy release in the decay of the massive top quark, the decay products come wide apart. In contrast the energy release in the light b or c quark decay is small, so that the decay products come together in a narrow cone – i.e. the charged lepton appears as a part of the decay quark jet. The isolated lepton signature provides a simple but very effective signature for top quark, first suggested in [17]. Using this signature the top quark search was carried out at the CERN $\bar{p}p$ collider and then at the Tevatron collider upto a mass limit of $m_t \simeq 90$ GeV [18].

With the luminosity upgrade of the Tevatron collider it has been possible now to extend the search to the mass range of $100 - 200$ GeV. A top quark in this mass range decays into a real W boson, so that one has a $2W$ final state, i.e.

$$t\bar{t} \to W^+W^-b\bar{b}. \tag{30}$$

The resulting signature for top quark and the corresponding background were first analysed in [19]. Requiring leptonic decay of both or one of the W bosons leads to an isolated dilepton or single lepton signature, i.e.

$$t\bar{t} \to \ell^+\ell^-\nu\bar{\nu}b\bar{b} \tag{31}$$

or

$$t\bar{t} \to \ell\nu b\bar{b}q\bar{q}'. \tag{32}$$

In either case there are several accompanying quark jets and a missing-p_T due to the escaping neutrino(s). The dilepton signature (31) is small in

size, since one has to pay the price of a small leptonic branching ratio of W ($\simeq 2/9$) twice. But it is relatively clean, since there is only a small background from the second order electroweak process

$$q\bar{q} \to W^+W^-. \tag{33}$$

In contrast the single lepton signature (32) is relatively large; but one has to contend with a much larger background from single W production along with QCD jets, e.g.

$$\bar{q}q \to Wgg \to \ell\nu j_1 j_2. \tag{34}$$

However the QCD jets are normally soft and besides one has to pay a price of α_s for each additional jet. In contrast the decay of a heavy $t\bar{t}$ pair automatically gives a large number of decay quark jets in (32), which are hard and well separated in angle. Consequently the background can be kept in control by suitable cuts on the number and hardness of the jets accompanying the isolated lepton [19-21].

Fig. 5 shows the predicted dilepton and single lepton signals from [19] for an integrated Tevatron collider luminosity of 100 pb^{-1}, which is relevant for its current run [22,23]. The dilepton signal is seen to be viable upto $m_t \simeq 150$ GeV. The single lepton signal (32) is shown separately for different numbers ($n = 2, 3, 4$) of accompanying jets.[3] The single lepton background from (33) and (34) are also shown for comparison. Modest jet hardness cuts of

$$\sum \vec{p}_{Tj} > 60 \text{ GeV}, \quad m_{jj} > 60 \text{ GeV}, \tag{35}$$

have been applied on the vector sum of the jet p_T's and the invariant mass of the two hardest jets. This is adequate to keep the background below the level of the $n \geq 2$ signal upto $m_t \simeq 150$ GeV. Moreover it is possible to achieve this all the way upto $m_t \simeq 200$ GeV using a tighter jet hardness ($\sum \vec{p}_{Tj}$) cut and restricting to $n \geq 3$, as noted in [19]. Similar results have been obtained in [20,21] using alternative forms of the jet hardness variable like the scalar sum of the jet p_T's [20] or the p_T's of the

[3]This separation depends to some extent on the choice of cone angle and p_T threshold of the jets. The cone angle used by the Tevatron experiments [22,23] are some what smaller than the conservative assumption of [19]. As a result the 3 and 4 jet contributions become comparable for $m_t = 150 - 200$ GeV.

two hardest jets [21]. Finally, the presence of a pair of b jets in the signal process can be used to separate it from the background, given a good b identification efficiency via a microvertex detector.

Recently the CDF and D$\emptyset$ experiments, working at the Tevatron collider, have identified a heavy top quark signal using the above mentioned techniques [22,23]. Their results are based on the integrated luminosities of 67 and 50 pb^{-1} respectively, i.e. about half the projected luminosity of $\sim$ 100 pb^{-1} for the current Tevatron run. The CDF experiment [22] uses b tagging via a silicon microvertex detector to separate the single lepton signal (32) from the QCD background (34), while the D$\emptyset$ experiment [23] achives this using the jet hardness criterion. Fig. 6 shows the CDF data for the W plus $\geq$ 4 jet events before b-tagging along with the predicted background [22]. The events are plotted against the reconstructed mass, i.e. the invariant mass of the W and a suitably chosen jet so that it nearly matches with the invariant mass of the three remaining jets. Although the background accounts for about 70% of the data, one sees a clear excess in the mass range of $\sim$ 175 GeV. Fig. 8 shows the corresponding events after b-tagging. The later improves the signal to background ratio significantly, while the signal size is reduced by the tagging efficiency factor of $\sim$ 40%. Thus a top quark signal of about a dozen events is clearly visible against a background of $\sim$ 7 events. The shape of the event distribution gives a top quark mass of

$$m_t = 176 \pm 8 \pm 10 \text{ GeV}, \tag{36}$$

where the 1st and 2nd errors correspond to the statistical and systematic uncertainties respectively. The $t\bar{t}$ cross-section estimated from the signal size,

$$\sigma_{t\bar{t}} = 6.8^{+3.6}_{-2.4} \text{ pb}, \tag{37}$$

is in agreement with the QCD prediction. The statistical significance of the CDF top quark signal after combining the single lepton and dilepton data is at the level of 4.8σ. The D$\emptyset$ experiment has given a top quark signal of comparable statistical significance and similar size of cross-section; but their mass estimate is less precise [23]; i.e.

$$m_t = 199^{+19}_{-21} \pm 22 \text{ GeV}. \tag{38}$$

Let me try to put the above result in perspective and make some future projections. As we have seen in the earlier sections, the top quark

search has been a long programme extending over the last fifteen years. The evidence for the existence and mass of the top quark has built up step by step from a large number of indirect experiments. The direct observation of the top quark signal at the Tevatron collider is of course the final step. It is also the most difficult one. Firstly we see from Fig. 5 that the relevant signal size for $m_t \sim 175$ GeV is only a few tenths of a *pb*. Compared with the $\bar{p}p$ total cross-section of ~ 100 mb, this is at the level of a few parts in a trillion. This is a thousand time smaller than the W and Z boson signals, observed a decade ago, which were a few parts in a billion. Secondly, the W and Z bosons had unmistakable leptonic signatures with practically no background. In contrast, the direct W production is an unavoidable background for the top quark signal, which is hard to suppress and impossible to eliminate. Thus one has to extricate the signal events of few parts in a trillion from the background of few parts in a billion. Finally it is the first example of identifying a new particle peak in a multijet in stead of a multiparticle channel. It may be noted here that the W and Z boson peaks are yet to be seen in a dijet channel at a hadron collider. One should bear these points in mind in order to appreciate the real significance of the top quark signal, observed at Tevatron.

At the same time it is fair to say that the current Tevatron result is a semifinal rather than the final step in the top quark search. For a 5σ signal by itself constitutes a promising rather than conclusive signal. The recent history of particle physics is replete with many examples of 5σ signals that have fallen by the way side. The reason the top quark signal is taken more seriously of course is that it falls in place with the indirect evidences, particularly from LEP (Fig. 3). Nonetheless there is a lot of scope for improvement and cross-checks on the direct top quark signal, which can be done with more data from the Tevatron collider. For instance, one can check the correlation between the event samples selected via b-tagging and via the jet hardness cut. Moreover one can supplement b-tagging by a jet hardness cut to improve upon the signal to background ratio shown in Fig. 7, at a cost to the signal size of course. Besides one should be able to get independent signals at $> 5\sigma$ levels in single lepton and dilepton (particularly $e\mu$) channels, and check their relative magnitudes with the universality prediction. Some of these can surely be done with the doubling of the data sample by the end of the current

run. Note however that one would still have only about two dozens of signal events. On the other hand the installation of the main injector following this run is expected boost the Tevatron luminosity further by an order of magnitude. Consequently the next run, scheduled for 1998, is expected to yield a data sample of a few hundred signal events. This will enable one to improve the signal to background ratio and perform various cross-checks, as indicated above. As a result one expects to see a conclusive signal for top from this data. Of course there will still be a lot of interesting top quark physics left for LHC and beyond.

6 Top Quark Physics at LHC and NLC

The top quark production cross-section at LHC is ~ 100 times larger than at the Tevatron collider energy. Fig. 8 shows the expected $t\bar{t}$ cross-section in the cleanest dilepton channel ($e\mu$) against the p_T of the softer lepton [24]. It corresponds to an integrated cross-section of $\sim 10^4$ fb in the $e\mu$ channel or equivalently $\sim 10^5$ fb in the single-lepton channel discussed above. Even with the low luminosity option of LHC (~ 10 fb/year), this would imply an annual rate of ~ 1 million top quark events - i.e. similar to the rate of Z events at LEP. Thus the LHC can serve as a top quark factory. This will enable one to study its decay properties in detail and to search for new particles in the top quark decay. In particular there has been a good deal of recent interest in the search for one such new particle, for which the top quark decay offers by far the best discovery limit – i.e. the charged Higgs boson $H^{\pm}$ of the supersymmetric standard model. Detailed signatures for $H^{\pm}$ search in the top quark decay at LHC have been studied in [25].

Of course the ultimate stage of the top quark physics will be reached at the next linear collider (NLC), a generic name for a e^+e^- machine with CM energy $\gtrsim 500$ GeV, which is hoped to follow LHC [26]. As we have already seen in eq. (24) above, the $t\bar{t}$ production cross-section would constitute about a quarter of the hadronic cross-section in a e^+e^- collider. The copious production rate and the clean environment of a e^+e^- machine would make it possible to measure top quark mass to an accuracy of 0.5 GeV and measure its life time. It may be noted here that the large mass of top implies a life time $\sim 10^{-23}$ sec.; which means that the top quark decays before hadronization. Consequently the spin

and polarisation of top can be measured from the kinematic distribution of its decay products. The polarisation information will be useful for studying CP violation effects in $t\bar{t}$ production. In particular this process is well suited to look for possible CP violation induced via the Higgs sector because of the large Higgs coupling to top. Of course the short life of top means there will be no toponium states to study. Nonetheless there is a wealth of information to be gained from the detailed study of $t\bar{t}$ production at the NLC.

It is a pleasure to dedicate this article to Haridasda, who has been a good friend and an elder brother to me for the last thirty years, on the occasion of his sixtieth birthday.

References

1. See any text on particle physics, e.g. F. Halen and A.D. Martin, Quarks and Lepton, John Wiley, New York (1984).
2. S.L. Wu, Proc. of 1987 Intl. Symp. on Lepton and Photon Int. at High Energies, North-Holland (1988).
3. V. Barger and S. Pakvasa, Phys. Lett. 81B, 195 (1979); G.L. Kane and M.E. Peskin, Nucl. Phys. B195, 29 (1982).
4. CLEO collaboration: A. Bean et al., Phys. Rev. D35, 3533 (1987).
5. D.P. Roy and S. Uma Sankar, Phys. Lett. 243B, 296 (1990).
6. ARGUS collaboration: H. Albercht et al., Phys. Lett. 192B, 245 (1987); CLEO collaboration: M. Artuso et al., Phys. Rev. Lett. 62, 2233 (1989).
7. Review of Particle Properties, Phys. Rev. D50, 1173-1826 (1994).
8. S. Pakvasa, D.P. Roy and S. Uma Sankar, Phys. Rev. D42, 3106 (1990)
9. D.P. Roy, in Particle Phenomenology in the 90's (Proc. of WHEPP-II, Calcutta, 1991), World Scientific (1992), p 30.
10. P.J. Franzini, Phys. Rep. 173, 1 (1989), and references therein.
11. CDF collaboration: F. Abe et al., Phys. Rev. Lett. 73, 220 (1994).
12. U. Amaldi et al., Phys. Rev. D36, 1385 (1987); G. Costa et al., Nucl. Phys. B297, 244 (1988); J. Ellis and G. Fogli, Phys. Lett. 232B, 139 (1989); P. Langacker, Phys. Rev. Lett. 63, 1920 (1989).
13. D. Schaile, Proc. of 27th Intl. Conf. on High Energy Physics, Glasgow, 1994, Vol. I, p 27 (Inst. of Physics Publishing, Bristol).
14. W. Hollik, Karlsruhe Preprint, KA-TP-2-1995 (1995).

15. VENUS collaboration: H. Yoshida et al., Phys. Lett. 198B, 570 (1987);
TOPAZ collaboration: J. Adachi et al., Phys. Rev. Lett. 60, 97 (1988);
AMY collaboration: H. Sagawa et al., Phys. Rev. Lett. 60, 93 (1988).

16. OPAL collaboration: M. Akrawy et al., Phys. Lett. 236B, 364 (1990);
ALEPH collaboration: D. Decamp et al., Phys. Lett. 236B, 511 (1990);
DELPHI collaboration: P. Abreu et al., Phys. Lett. 242B, 536 (1990).

17. R.M. Godbole, S. Pakvasa and D.P. Roy, Phys. Rev. Lett. 50, 1539 (1983);
V. Barger, A.D. Martin and R.J.N. Phillips, Phys. Rev. D28, 145 (1983).

18. CDF collaboration: F. Abe et al., Phys. Rev. D45, 3921 (1992).

19. S. Gupta and D.P. Roy, Z. Phys. C39, 417 (1988).

20. H. Baer, V. Barger and R.J.N. Phillips, Phys. Rev. D39, 3310 (1989).

21. R. Wagner et al., Top quark working group report in Physics at the Fermilab in the 1990's (Proc. of the Breckenbridge Workshop), World Scientific (1990), p 181.

22. CDF collaboration: F. Abe et al., Phys. Rev. Lett. 74, 2626 (1995).

23. DØ collaboration: S. Abachi et al., Phys. Rev. Lett. 74, 2632 (1995).

24. N.K. Mondal and D.P. Roy, Phys. Rev. D49, 183 (1994).

25. D.P. Roy, Phys. Lett. 277B, 183 (1992); 283B, 403 (1992).

26. See e.g. Proc. of the Workshop "e^+e^- collisions at 500 GeV: The Physics Potential", DESY Pub. 92-123A/B (1992).

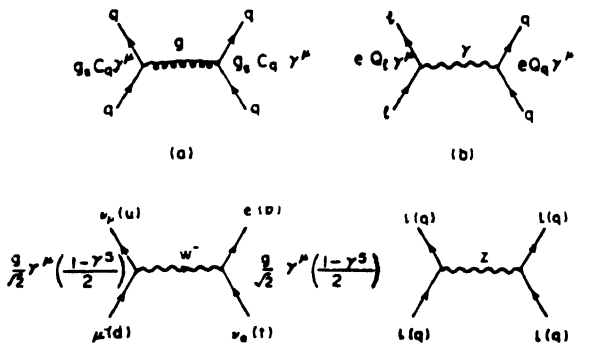

Fig. 1. Basic interactions of quarks and leptons. a, Strong. b, Electromagnetic. c, Charged current weak. d, Neutral current weak.

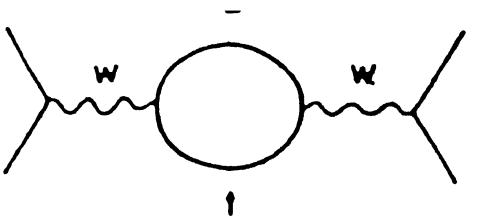

Fig. 2. Radiative correction to the W boson mass arising from the $t\bar{b}$ loop.

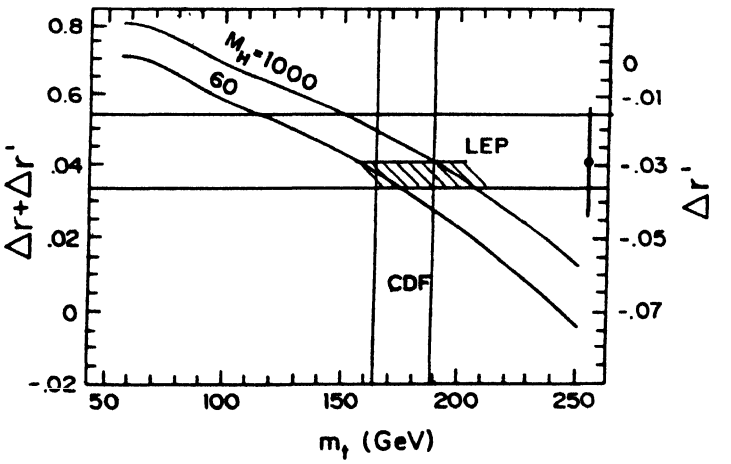

Fig. 3. Radiative correction as a function of top mass for $M_H = 60$ and 1000 GeV. The 1σ bound from M_Z and $\sin^2\theta_W$ are shown for three different estimates of $\sin^2\theta_W$: from M_W/M_Z (horizontal band), from νN scattering (point) and finally from the precission measurement of Z parameters at LEP (hatched band) [13,14]. The direct estimate of top mass from the CDF experiment [22] is also shown for comparison.

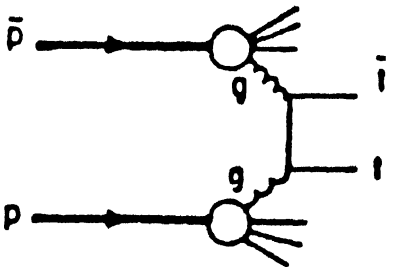

Fig. 4. Top quark production in $\bar{p}p$ (pp) collision via gluon-gluon fusion.

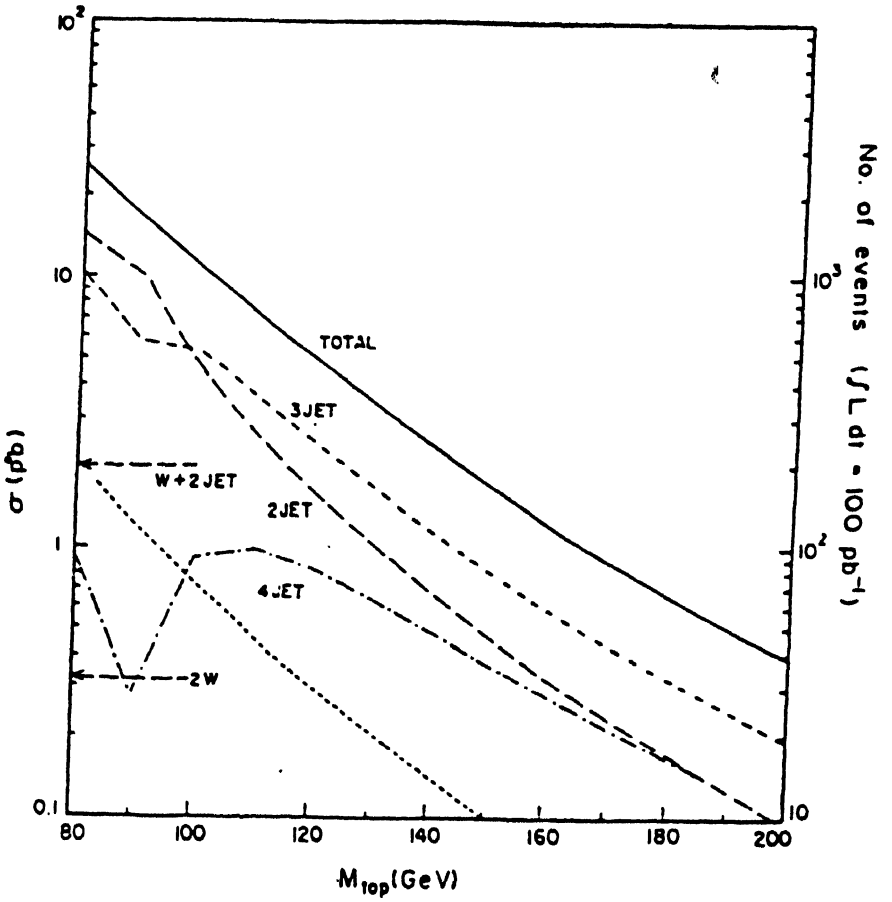

Fig. 5. Top quark contribution to the isolated lepton plus n-jet events and also dilepton events (dotted line) shown for the typical energy (2 TeV) and luminosity (100 pb^{-1}) of the Tevatron collider. The background to the 2-jet events from W plus 2-jet and W pair production processes are also shown. [19]

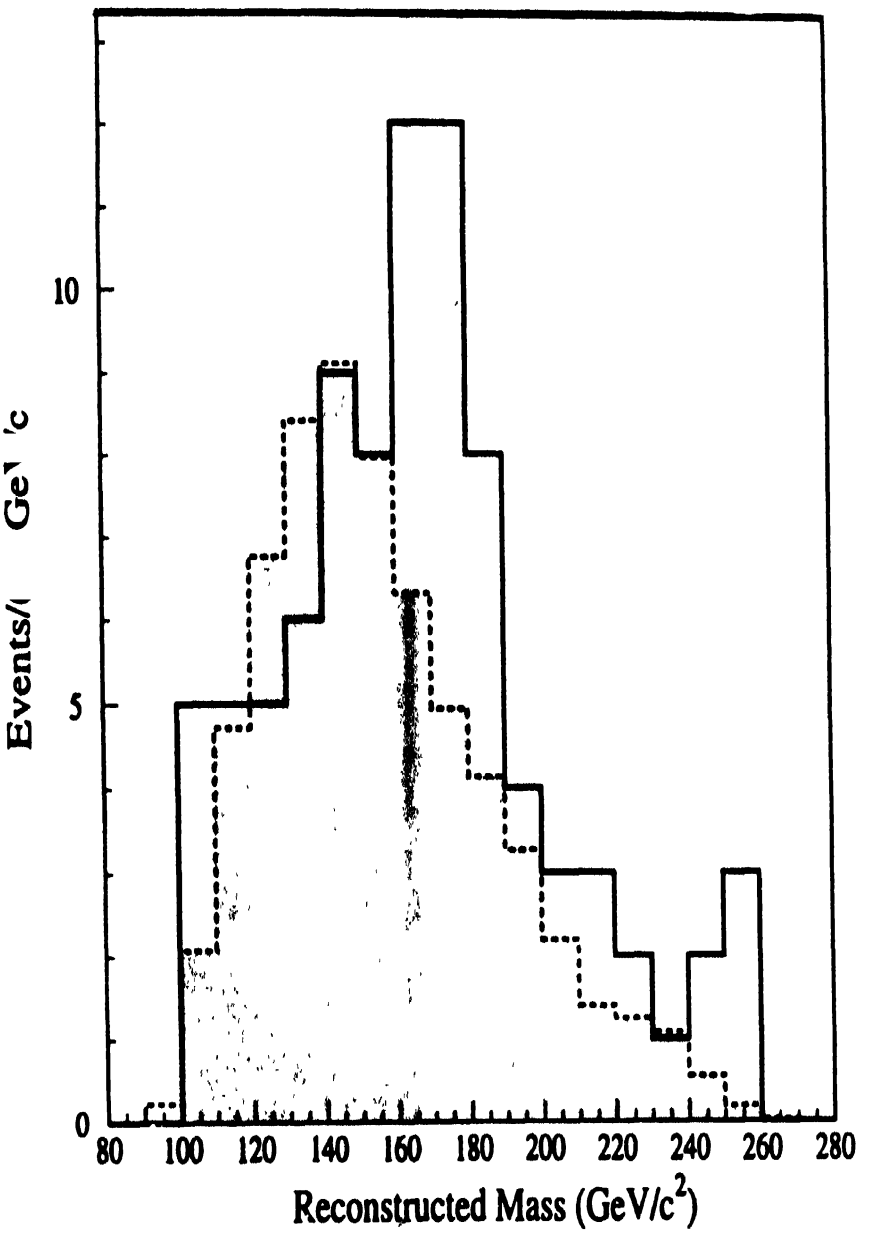

Fig. 6. Reconstructed mass distribution for the $W+ \geq 4$-jet sample prior to b-tagging (solid). Also shown is the background distribution (shaded), with the normalization constrained to the calculated value. [22]

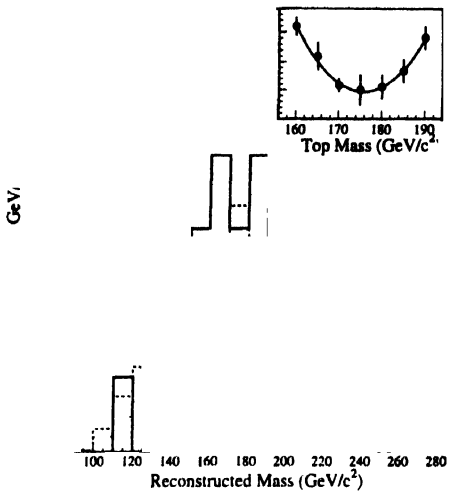

Fig. 7. Reconstructed mass distribution for the b-tagged $W+ \geq 4$-jet events (solid). Also shown are the background shape (dotted) and the sum of background plus $t\bar{t}$ Monte Carlo for $M_{top} = 175$ GeV/c^2 (dashed), with the background constrained to the calculated value, $6.9^{+2.5}_{-1.9}$ events. The inset shows the likelihood fit used to determine the top mass. [22]

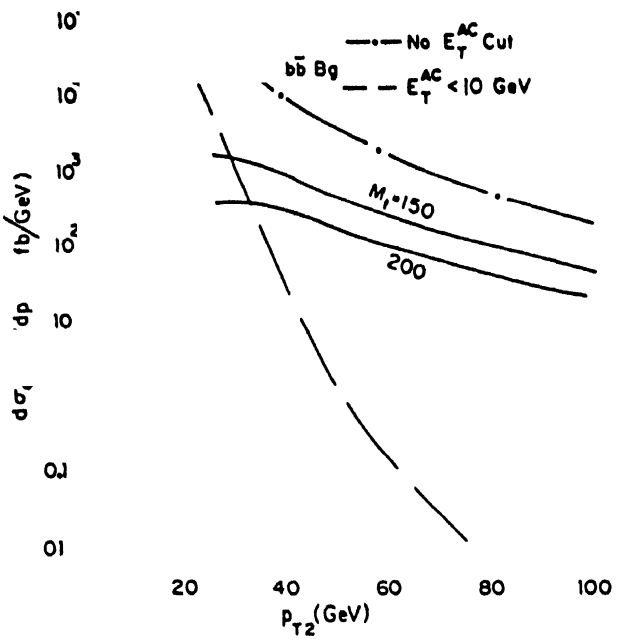

Fig. 8. The expected $t\bar{t}$ signal at LHC in the cleanest ($e\mu$) channel shown against the p_T of the 2nd (softer) lepton. The $b\bar{b}$ background with and without the isolation cut are also shown. [24]